ENZYMATIC DIGESTION COMBINED WITH μFT-IR IMAGING FOR RECOVERY AND CHARACTERISATION OF POLYMER PARTICLES FROM *MYTILUS GALLOPROVINCIALIS* TISSUE

SEVDALINA TURMANOVA[1], YANCHO HRISTOV[1], DIMITRINA KIRYAKOVA[1,*], EMILIYA IVANOVA[2], PLAMENA ATANASOVA[1], GANKA KOLCHAKOVA[1], ANTONIYA ILIEVA[3], AND ELENA MOLLOVA[2]

[1] Department of Materials Science, Burgas State University "Prof. Dr. Assen Zlatarov", 1 Y. Yakimov Str., Burgas 8010, Bulgaria
[2] Department of Ecology and Environmental Protection, Burgas State University "Prof. Dr. Assen Zlatarov", 1 Y. Yakimov Str., Burgas 8010, Bulgaria
[3] Department of Chemical Technologies, Burgas State University "Prof. Dr. Assen Zlatarov", 1 Y. Yakimov Str., Burgas 8010, Bulgaria
* Corresponding author: dskiryakova@abv.bg

ABSTRACT

Microplastic contamination in marine organisms requires analytical approaches capable of efficiently removing biological matrices while preserving polymer integrity. Building upon previous work identifying enzymatic digestion as a suitable treatment method, the present study applies a pancreatic enzyme protocol (Kreon®25000) to recover polymer particles from *Mytilus galloprovincialis* tissue and to evaluate particle characteristics by μFT-IR imaging. Frozen mussel tissue (2 g) was artificially spiked with reference particles of PVC, HDPE, PA, and PET and subjected to enzymatic digestion under controlled conditions. Digestion removed 99.8% of the biological matrix, allowing subsequent filtration, microscopic inspection, and spectroscopic identification. A total of 2334 particles were detected. Recovery varied among polymers, with HDPE showing the highest numerical recovery and PET the lowest. Particle size distributions differed markedly: HDPE, PA, and PVC were dominated by particles <50 μm, whereas PET particles were predominantly larger. Morphological analysis revealed irregular fragment-like shapes across all polymer types. μFT-IR imaging enabled polymer identification and spatial mapping, revealing heterogeneous particle distribution and localized clustering patterns on filter surfaces. Comparison of ATR-FTIR reference spectra with μFT-IR spectra obtained after digestion confirmed preservation of diagnostic polymer bands, indicating that enzymatic treatment did not alter polymer chemical structure. The results demonstrate that enzymatic digestion combined with μFT-IR imaging provides a reliable and polymer-preserving workflow for microplastic analysis in marine biological matrices. The findings highlight the influence of particle size and spatial distribution on recovery and detection, underscoring the importance of standardized imaging strategies for accurate quantification.

Keywords: contamination control; microplastic analysis; marine biota; size classification; spatial distribution; spectroscopic identification

Introduction

Microplastics (MPs) are synthetic polymer particles introduced into the marine environment through long-term accumulation and subsequent fragmentation of plastic materials (Barnes et al. 2009; Kalogerakis et al. 2017; Yang et al. 2021). They are typically defined as particles smaller than 5 mm and occur in various morphological forms, including fragments, fibers, films, and spheres. Their physicochemical properties vary depending on polymer type, degree of weathering, and environmental conditions (Tirkey and Upadhyay 2021; Golmohammadi et al. 2023; U.S. Environmental Protection Agency 2024). Based on their origin, microplastics are classified as primary particles manufactured at microscopic size for specific applications and secondary particles formed through mechanical, photochemical, and thermal degradation of larger plastic debris (Duis and Coors 2016; Cverenkárová et al. 2021; Song et al. 2024). MPs have been detected throughout the marine environment, including the water column, sediments, and marine biota (Van Cauwenberghe et al. 2015; Sunny et al. 2025).

Due to their filter-feeding behavior, bivalve mollusks, including *Mytilus galloprovincialis*, efficiently retain suspended particles from the surrounding environment, including microplastic fragments and fibers (Pizzurro et al. 2022, 2023; Kovačić et al. 2024). This species is widely distributed in coastal zones and exhibits limited mobility, making it a suitable bioindicator for assessing local pollution levels (Pizzurro et al. 2023; Mihailov et al. 2025). The accumulation of microplastic particles in *M. galloprovincialis* tissues provides valuable insight into the exposure of coastal ecosystems to synthetic polymers.

The analysis of microplastics in biological tissues is associated with methodological limitations, particularly at the stage of organic matter removal. Frequently used acidic and alkaline treatments may affect the surface structure and chemical composition of certain polymers, creating conditions for partial degradation or analytical losses (Pfeiffer and Fischer 2020; Di Fiore et al. 2024; Tuuri et al. 2024). The lack of harmonized protocols further limits the possibility for direct comparability between different studies (Hermsen et al. 2018; Al-Azzawi et al. 2020).

Turmanova, S., Hristov, Y., Kiryakova, D., Ivanova, E., Atanasova, P., Kolchakova, G., Ilieva, A., Mollova, E.: Enzymatic digestion combined with μFT-IR imaging for recovery and characterisation of polymer particles from *Mytilus galloprovincialis* tissue
European Journal of Environmental Sciences, Vol. 16, No. 1, pp. 41–51
https://doi.org/10.14712/23361964.2026.3

Enzymatic digestion has emerged as a promising alternative, allowing selective removal of biological material under controlled conditions with minimal impact on polymer structure (Mo et al. 2018; von Friesen et al. 2019; Di Fiore et al. 2024; Khan and Zaidi 2025). This approach facilitates subsequent spectroscopic identification and morphological characterization of particles (Chen et al. 2020; Morgado et al. 2021).

Previous research systematically evaluated enzymatic, acidic, and alkaline digestion protocols for the removal of biological matrices in *Mytilus galloprovincialis*, identifying enzymatic digestion as the most reliable approach for preserving polymer integrity and ensuring high recovery efficiency (Turmanova et al. 2026). Building upon these findings, the present study applies the previously validated enzymatic protocol to mussel tissue artificially spiked with reference polymer particles and performs detailed μFT-IR imaging analysis. The study focuses on polymer identification, particle morphology, size distribution, and spatial distribution on filters, thereby advancing methodological reliability in microplastic analysis of marine biota. The aim of this study was to evaluate the recovery, characterization, and spatial distribution of selected polymer particles from Mytilus galloprovincialis tissue following enzymatic digestion using μFT-IR imaging.

Materials and Methods

Materials

Black Sea mussels, *Mytilus galloprovincialis*, collected from the Burgas Bay (Black Sea, Bulgaria), were used as model biological material in the present study. Mussels were stored frozen at −20 °C until analysis. Reference polymer particles were used to simulate microplastic contamination: polyvinyl chloride (PVC, 100–200 μm), high-density polyethylene (HDPE, 100–500 μm), polyamide (PA, 100–200 μm), and polyethylene terephthalate (PET, 100–250 μm). Enzymatic digestion was performed using Kreon®25000 (Abbott Laboratories GmbH, Germany), a pancreatic enzyme containing lipase (25,000 Ph. Eur units), amylase (18,000 Ph. Eur units), and protease (1,000 Ph. Eur units).

Sample preparation and polymer spiking

Frozen *Mytilus galloprovincialis* tissue (2.0 g) was used for the experiment. Samples were artificially spiked with known masses of microplastic particles representing four polymer types: polyvinyl chloride (PVC), high-density polyethylene (HDPE), polyamide (PA), and polyethylene terephthalate (PET). Particle size ranges were 100–200 μm for PVC and PA, 100–500 μm for HDPE, and 100–250 μm for PET. Separate samples were prepared for each polymer type, with only one polymer introduced per sample to allow polymer-specific recovery assessment and to prevent spectral overlap. A procedural control without added polymers was processed in parallel to verify background cleanliness. All handling procedures were conducted under contamination-controlled conditions, and samples were covered when not in use.

Enzymatic digestion using Kreon®25000

Enzymatic digestion was performed using Kreon® 25000 (Abbott Laboratories GmbH, Germany). A total of 0.125 g of Kreon®25000 was dissolved in 20 mL of 1 M Tris-HCl buffer solution (pH 8.0), corresponding to the optimal activity range of pancreatic enzymes (Berdutina et al. 2000; von Friesen et al. 2019). The spiked mussel samples were added to the enzyme solution and incubated at 37.8 °C for 2 hours under constant stirring (300 rpm). These conditions were selected based on a previously optimized enzymatic protocol validated for *Mytilus galloprovincialis,* which demonstrated efficient biological matrix removal (99.8%) (Turmanova et al. 2026).

Filtration

Following enzymatic digestion, the resulting solutions were vacuum-filtered through metal filters with a pore size of 5 μm. Filters were rinsed with ultrapure water to remove residual reagents, dried at 40 °C, and stored in sealed containers until further analysis.

Microscopic inspection of filters

Filters were examined using a BSCOPE BS.1153-EPLH microscope (Euromex, Netherlands) to document representative polymer particles retained on the filters after digestion. Micrographs were captured at 40× magnification to illustrate particle morphology and surface features. Optical microscopy was used for particle visualization, while polymer identification was confirmed by μFT-IR analysis.

Identification of polymer particles by μFT-IR imaging

Prior to μFT-IR analysis, particles retained on the metal filters were carefully transferred onto Anodisc membrane filters (0.2 μm) to improve infrared transmission and enhance spectral quality during imaging. Polymer particles were analyzed using a μFT-IR imaging microscope (LUMOS II, Bruker Optik GmbH, Germany). The instrument was equipped with a focal plane array (FPA) detector (32 × 32 pixels) providing a spatial resolution of 5 μm. Spectral imaging was performed in the range of 1000–4000 cm^{-1} with a spectral resolution of 5 cm^{-1}. Measurements were conducted in reflection mode, and background spectra were collected prior to each analysis. The effective spectral region used for polymer identification ranged approximately from 1200 to 3500 cm^{-1}.

μFT-IR data were processed using Purency Microplastics Finder software for automated particle detection and polymer identification. Particles were classified as polymer particles when the spectral match met the acceptance criteria defined in the reference spectral libraries. Only particles with an acceptable spectral match score above 70% were considered confirmed microplastics. The spatial coordinates of identified particles were recorded during imaging and used for subsequent analysis of particle morphology and spatial distribution on the filters. The µFT-IR imaging system also enabled visualization of the overall filter surface, allowing assessment of residual biological material and particle retention after digestion.

ATR-FTIR Spectroscopy of polymer particles

Reference polymer particles (HDPE, PA, PVC, and PET) were analyzed using an ALPHA II FT-IR spectrometer (Bruker Optik GmbH, Germany) equipped with a Platinum ATR module and a diamond crystal. Spectra were recorded in the range of 400–4000 cm^{-1} at a spectral resolution of 4 cm^{-1} and averaged over 32 scans to improve the signal-to-noise ratio. The resulting spectra served as reference profiles for comparison with µFT-IR spectra obtained from filter-retained particles after enzymatic digestion. Each polymer type was analyzed separately prior to use as reference material and re-analyzed after enzymatic digestion under the same ATR-FTIR conditions to verify spectral consistency and confirm that the digestion procedure did not alter polymer chemical structure.

Particle characterization and data analysis

Particle characterization was performed based on µFT-IR imaging data. Particle size was determined as the equivalent circular diameter calculated from the projected particle area. Particles were grouped into size classes (< 50 µm, 50–100 µm, 100–300 µm, and > 300 µm) to evaluate size distribution.

Particle morphology was assessed using shape descriptors derived from imaging data. Particles were classified as irregular fragments based on aspect ratio and particle outline. Only particles larger than 5 µm were included in the analysis.

The spatial coordinates obtained from µFT-IR imaging were used to generate spatial distribution and density maps of polymer particles on the filters. Descriptive statistical analysis (particle counts, size distribution, and percentage distribution by size class) and graphical representations were performed using Microsoft Excel (Microsoft Corp., USA).

Quality assurance and contamination control

All glassware and tools were thoroughly rinsed with filtered ultrapure water prior to use. Sample preparation

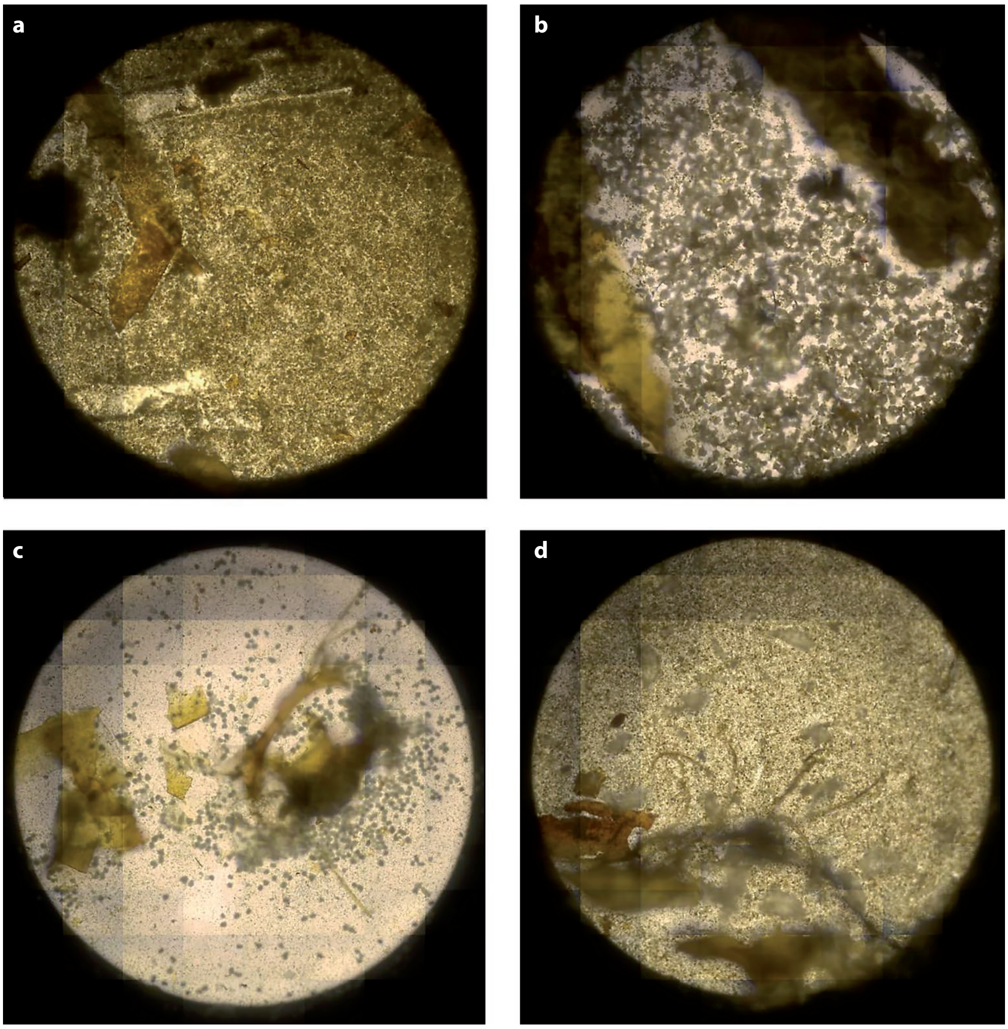

Fig. 1 Representative filter images after enzymatic digestion showing (a) HDPE, (b) PA, (c) PVC and (d) PET.

Table 1 Recovery and size characteristics of detected polymers.

Polymer	Added mass (mg)	Detected particles (n)	Particles per mg	Median size (µm)	Size range (µm)
HDPE	12.38	1107	89	15.4	0.9–64.8
PA	15.47	827	53	27.0	1.6–110.4
PVC	17.47	350	20	26.9	2.4–146.6
PET	8.55	50	5	70.7	8.1–275.5

and filtration were conducted in a clean working environment, and samples were covered whenever possible to minimize contamination.

Results and Discussion

Recovery and detection of polymer particles

Polymer particles representing HDPE, PA, PVC, and PET were successfully detected, and identified from *Mytilus galloprovincialis* mussel tissue following enzymatic digestion using the previously validated Kreon®25000 protocol. The digestion effectively removed the biological matrix while preserving polymer integrity, enabling subsequent microscopic and µFT-IR identification. µFT-IR imaging of the filters confirmed clear retention of polymer particles on the filter surface, with only minimal residual biological material remaining (Fig. 1).

A total of 2334 particles were detected across all polymer types (Table 1). Recovery efficiency differed among polymers, reflecting differences in particle size distribution and material properties. HDPE exhibited the highest number of detected particles (1107), followed by PA (827) and PVC (350), while PET showed substantially lower recovery (50). When normalized to the added polymer mass, recovery ranged from 5 to 89 particles per mg, with HDPE showing the highest recovery efficiency and PET the lowest. The lower numerical recovery of PET is consistent with its larger particle size distribution and higher density, relative to polyolefins (Faszczewska et al. 2026), which can influence particle retention and detectability during filtration and imaging.

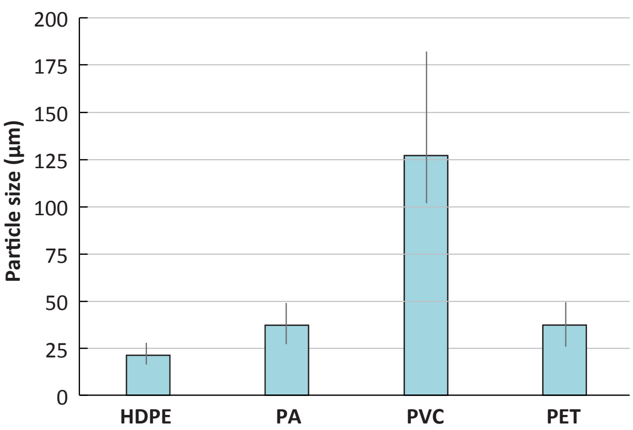

Fig. 2 Particle size distribution of HDPE, PA, PVC and PET particles detected after enzymatic digestion.

High recovery rates observed for HDPE and PA support the suitability of enzymatic digestion for efficient removal of organic tissue while preserving polymer particles. This observation is consistent with previous studies reporting that enzymatic digestion effectively removes biological material and minimizes polymer alteration compared with strong chemical treatments (Karami et al. 2017; Prata et al. 2019). The polymer-dependent differences in recovery are consistent with previous studies indicating that particle size, density, and polymer properties influence microplastic detection and recovery in biological matrices (Cole et al. 2014; Dehaut et al. 2016).

Particle size distribution

Particle size analysis revealed pronounced differences among polymer types (Table 1 and Fig. 2). Median particle sizes ranged from 15.4 µm for HDPE to 70.7 µm for PET, indicating substantial variability in particle dimensions after digestion and filtration.

HDPE particles were predominantly small, with 96% measuring < 50 µm, while only 4% fell within the 50–100 µm size class. Similarly, PVC and PA particles were largely within the smallest size fraction, with 69% and 71% < 50 µm, respectively. In contrast, PET exhibited a markedly different size distribution, with only 14% < 50 µm, while 46% and 40% of particles occurred in the 50–100 µm and 100–300 µm ranges, respectively (Table 2).

The predominance of smaller particles among HDPE, PA, and PVC reflects both the initial particle size characteristics and possible size reduction during sample handling and processing. Smaller particles are also more readily retained on filters and detected by µFT-IR imaging, contributing to their higher representation in the dataset.

Conversely, the larger size distribution observed for PET is consistent with its higher mechanical rigidity and resistance to fragmentation reported for polyester polymers (Andrady 2011). The lower proportion of small PET particles may also contribute to its reduced recovery ef-

Table 2 Percentage distribution of detected particles by size class.

Size class (µm)	HDPE	PA	PVC	PET
< 50	96%	71%	69%	14%
50–100	4%	23%	21%	46%
100–300	0%	6%	10%	40%
> 300	0%	0%	0%	0%

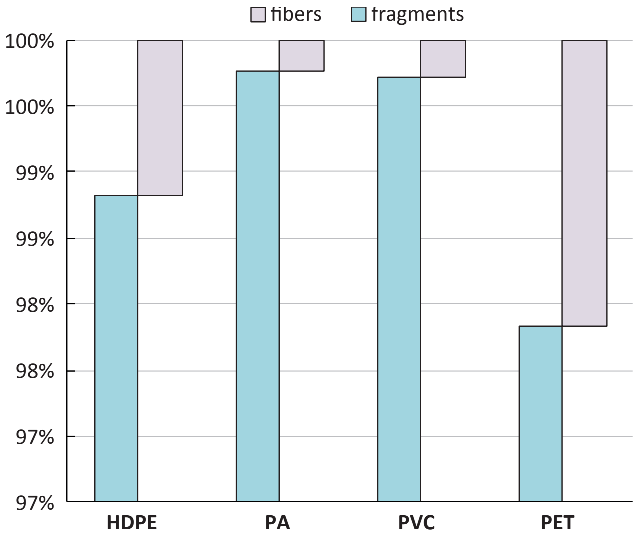

Fig. 3 Morphological distribution of HDPE, PA, PVC and PET particles detected after enzymatic digestion.

ficiency, as larger particles are more prone to loss during transfer and handling steps. The dominance of particles < 50 µm is consistent with previous microplastic recovery studies in biological matrices, where small particles represent the dominant fraction detected after digestion and filtration (Cole et al. 2014; Li et al. 2015). This size range is of particular ecological relevance, as smaller microplastics exhibit higher bioavailability and increased potential for trophic transfer.

Overall, these findings demonstrate that the enzymatic digestion protocol enables recovery and detection of polymer particles across a broad size spectrum while maintaining size characteristics necessary for reliable quantitative analysis.

Morphological characteristics of recovered polymer particles

Microscopic examination revealed that the recovered polymer particles exhibited irregular shapes and heterogeneous surface features characteristic of fragment-like microplastics. Most particles were classified as irregular fragments rather than fibers or films. Morphological differences were observed among polymer types. HDPE particles appeared predominantly as angular fragments, while PA particles showed more compact shapes with smoother edges. PVC particles exhibited irregular geometry with varied opacity, whereas PET particles were generally larger and more compact, often displaying

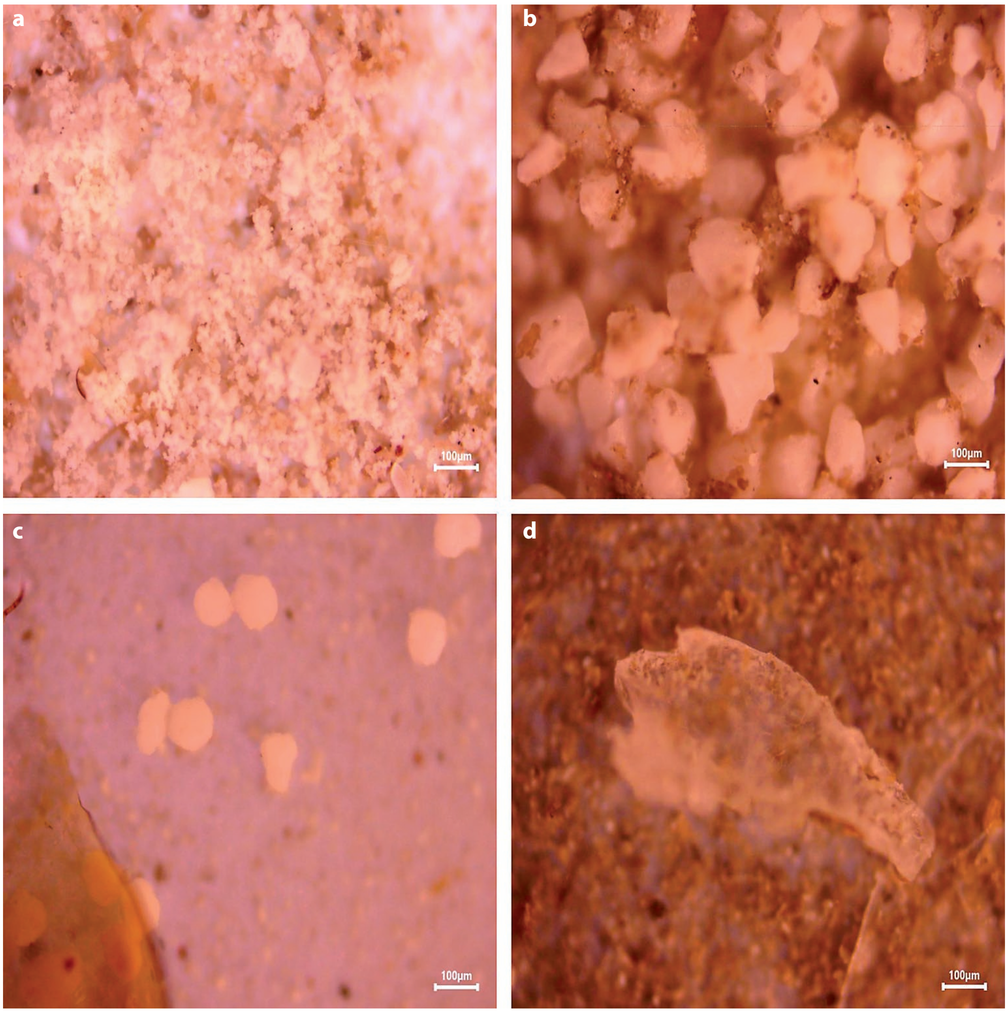

Fig. 4 Representative optical micrographs of polymer particles retained on filters after enzymatic digestion showing (a) HDPE, (b) PA, (c) PVC and (d) PET.

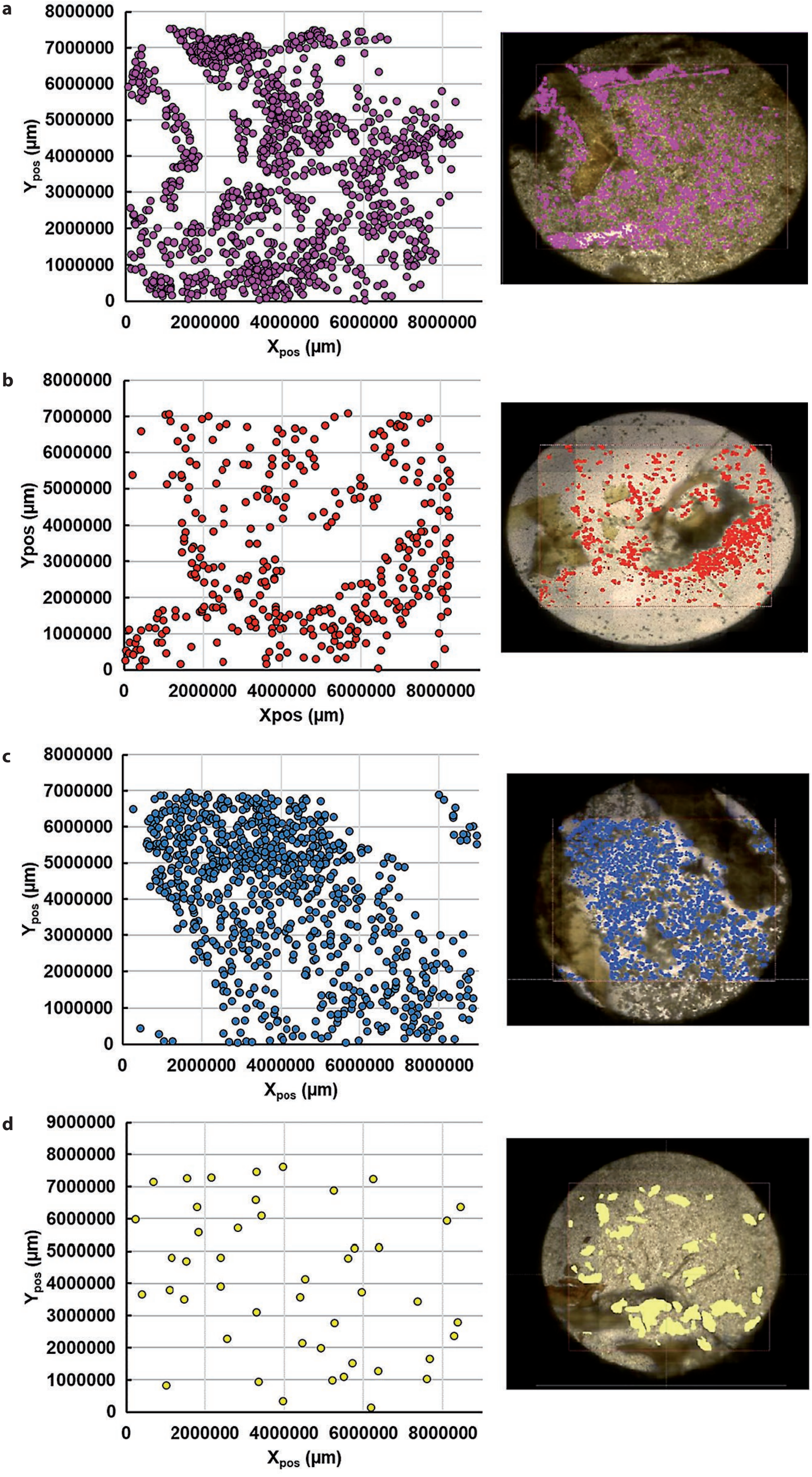

Fig. 5 µFT-IR imaging maps showing the spatial distribution and polymer identification of particles on filter surfaces: (a) HDPE, (b) PA, (c) PVC and (d) PET.

smoother surfaces and well-defined edges. Quantitative analysis of particle morphology confirmed the predominance of irregular fragments across all polymer types (Fig. 3). Shape descriptors derived from μFT-IR imaging data indicated that most particles had aspect ratios characteristic of fragment-like particles rather than elongated structures.

Representative optical micrographs illustrating the morphology and surface characteristics of the recovered particles are presented in Fig. 4a–d, highlighting differences in transparency, surface features, and edge definition among polymer types.

The predominance of irregular fragment-like shapes is consistent with morphologies commonly reported for environmental secondary microplastics (Cole et al. 2011; Hidalgo-Ruz et al. 2012). No visible surface degradation, melting, or structural alteration was observed following enzymatic digestion, indicating that the digestion protocol preserved polymer morphology. The observed variability in particle morphology and size suggests that particle shape may influence settling behavior and spatial distribution on the filters, which is further examined in the following section.

Spatial distribution and clustering patterns of polymer particles

Spatial analysis based on μFT-IR imaging coordinates revealed heterogeneous distribution patterns of polymer particles across the filter surfaces (Fig. 5 and Fig. 6). Scatter maps showed that particles were not uniformly dispersed but instead formed localized clusters and density gradients. HDPE particles, characterized by their small size and high abundance, appeared relatively evenly distributed across the filter surface. In contrast, PA and PVC particles showed moderate clustering, with localized accumulations observed in specific regions. PET particles, which were generally larger and less numerous, appeared in discrete areas rather than evenly distributed.

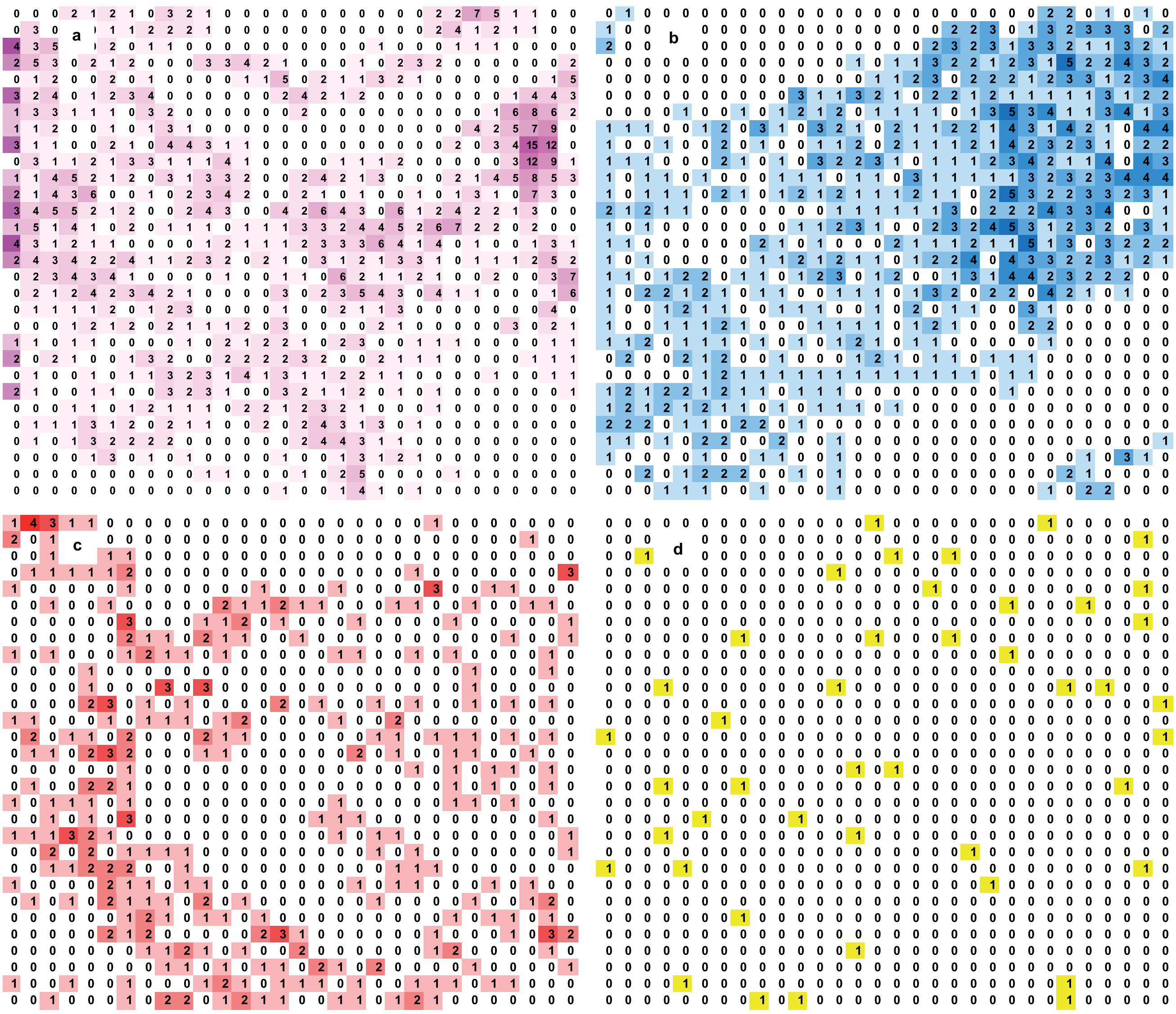

Fig. 6 Density maps showing spatial clustering and concentration patterns of polymer particles on filters after enzymatic digestion: (a) HDPE, (b) PA, (c) PVC and (d) PET.

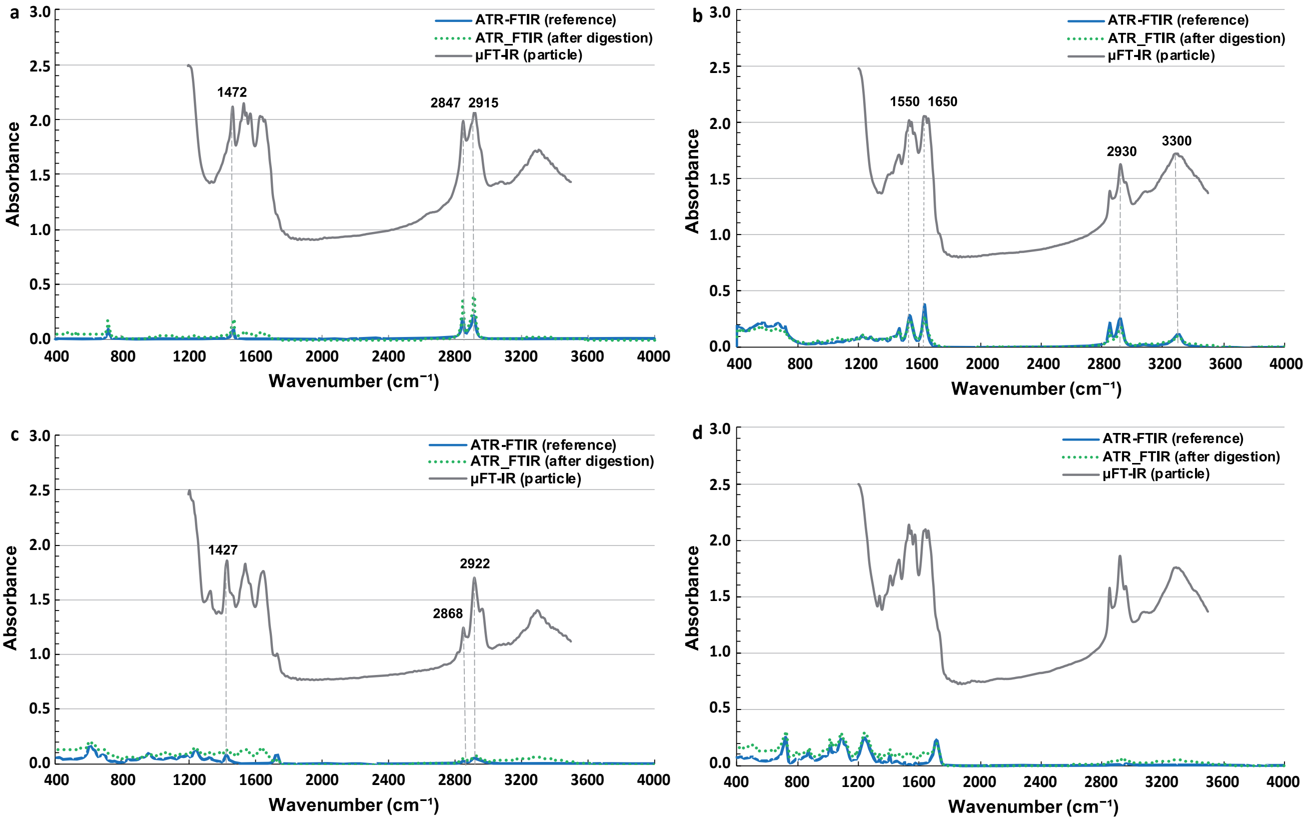

Fig. 7 Comparative ATR-FTIR reference spectra recorded before and after digestion and corresponding μFT-IR spectra of HDPE (a), PA (b), PVC (c) and PET (d) particles recovered following enzymatic digestion.

Density maps further highlighted these spatial trends, revealing zones of increased particle concentration (Fig. 6). Such heterogeneity likely reflects hydrodynamic processes during vacuum filtration, particle-particle interactions, and differences in settling behavior influenced by particle size and morphology. Non-uniform particle deposition on filter membranes has been reported in previous microplastic studies and represents an important methodological consideration, particularly when only subareas of a filter are analyzed, as this may affect quantitative estimates (Löder et al. 2017; Mintenig et al. 2019). Spatial clustering may influence quantitative estimates and should therefore be considered when designing imaging strategies. Overall, spatial mapping indicates that particle size and morphology may influence distribution behavior during filtration, reinforcing the importance of whole-filter imaging or standardized scanning protocols in microplastic analysis.

Spectroscopic identification and polymer integrity

Polymer identity was confirmed through comparison of μFT-IR spectra obtained from recovered particles with ATR-FTIR reference spectra recorded prior to enzymatic digestion (Fig. 7a–d). All four polymers exhibited characteristic absorption bands consistent with their known chemical structures. For HDPE, strong C–H stretching vibrations were observed in the region of 2848–2915 cm^{-1} (Fig. 7a), along with characteristic bending vibrations near 1470 and 720 cm^{-1} (Campanale et al. 2023; Circelli et al. 2024). PA particles displayed prominent amide I and amide II bands around 1650 and 1550 cm^{-1}, respectively (Fig. 7b), as well as N–H stretching vibrations near 3300 cm^{-1} (Narayanan and Janardhanan 2024; Schwab et al. 2024). PVC spectra (Fig. 7c) were characterized by C–Cl related absorptions in the fingerprint region between 600–700 cm^{-1} (Fernández-Sanmartín et al. 2024), while PET showed a distinct ester carbonyl band near 1715–1730 cm^{-1} (Fig. 7d) and aromatic ring vibrations in the 1400–1600 cm^{-1} range (Lujic et al. 2025).

The preservation of diagnostic absorption bands indicates that the enzymatic digestion procedure did not induce detectable chemical alteration of the polymers. Enzymatic digestion selectively degrades biological proteins, lipids, and carbohydrates (Mo et al. 2018; von Friesen et al. 2019; Di Fiore et al. 2024; Khan and Zaidi 2025) while leaving synthetic polymers structurally intact, in contrast to strong oxidative or acidic treatments that may cause surface oxidation or chain scission (Karami et al. 2017; Prata et al. 2019). Minor differences between ATR-FTIR and μFT-IR spectra may arise from differences in measurement geometry (ATR contact mode versus reflection imaging), particle thickness, surface roughness, and scattering effects associated with filter-based measurements, as discussed in vibrational microspectroscopy studies (Käppler et al. 2016). Such differences do not indicate chemical degradation but rather methodological variability inherent to spectroscopic techniques. The strong spectral agreement between reference and recovered particles demonstrates the suitability of the combined enzymatic digestion and μFT-IR imaging approach for accurate polymer identification in *Mytilus galloprovincialis* and similar marine biological matrices.

Methodological implications and study limitations

The present study demonstrates that enzymatic digestion using Kreon®25000 combined with μFT-IR imaging provides a reliable workflow for the recovery, identification, and characterization of polymer particles from *Mytilus galloprovincialis* mussel tissue. The protocol effectively removed biological material while preserving particle morphology and chemical integrity, enabling robust spectroscopic confirmation and spatial analysis.

Several methodological insights emerge from the results. First, particle size strongly influences detectability and numerical recovery. Polymers dominated by smaller size fractions (e.g., HDPE) yielded higher particle counts per unit mass, whereas larger particles (e.g., PET) resulted in lower numerical abundance despite comparable mass addition. This highlights the importance of considering both particle number and size distribution when evaluating recovery efficiency. Second, spatial clustering observed on filters indicates that particle deposition during vacuum filtration is not entirely uniform. Such heterogeneity may introduce variability if only partial areas of the filter are analyzed. Whole-filter imaging or standardized scanning strategies are recommended to minimize sampling bias, as emphasized in methodological studies on representative microplastic analysis (Löder et al. 2017). Third, the preservation of diagnostic FT-IR bands confirms that enzymatic digestion is polymer-compatible and avoids the chemical alterations sometimes associated with strong oxidative or acidic digestion protocols (Karami et al. 2017; Prata et al. 2019).

Despite these strengths, certain limitations should be acknowledged. The present study was conducted using controlled spiking experiments, with one analyzed filter per polymer type. While this design allows clear evaluation of polymer recovery and integrity, it does not address environmental variability or replicate-based statistical uncertainty. Future studies should incorporate multiple replicates and environmentally aged particles to further validate the robustness of the method under complex real-world conditions. Additionally, detection efficiency decreases for particles approaching the spatial resolution limit of μFT-IR imaging, potentially leading to underestimation of the smallest microplastic fraction (Käppler et al. 2016).

Overall, the findings support enzymatic digestion combined with μFT-IR imaging as a robust and polymer-preserving approach for microplastic analysis in biological matrices, while highlighting the importance of standardized imaging strategies and replication in future investigations.

Conclusion

This study demonstrates that enzymatic digestion using Kreon®25000 provides an effective and polymer-preserving approach for the recovery and identification of microplastic particles from *Mytilus galloprovincialis* tissue. The protocol achieved efficient removal of the biological matrix while maintaining particle morphology and chemical integrity, enabling reliable microscopic and spectroscopic analysis. Recovery efficiency varied among polymers and was strongly influenced by particle size and material properties. HDPE and PA exhibited higher numerical recovery, whereas PET showed lower particle counts, likely due to larger particle size and higher density. Size distribution analysis revealed dominance of particles <50 μm for HDPE, PA, and PVC, while PET particles were predominantly larger. μFT-IR imaging enabled accurate polymer identification and spatial mapping, revealing heterogeneous particle deposition and localized clustering patterns on filter surfaces. Morphological analysis confirmed the predominance of irregular fragment-like particles. Comparison of ATR-FTIR reference spectra with μFT-IR spectra obtained after digestion confirmed preservation of diagnostic polymer bands, demonstrating that enzymatic treatment did not induce detectable chemical changes. Overall, the combined use of enzymatic digestion and μFT-IR imaging represents a reliable workflow for microplastic analysis in marine biological matrices. The findings highlight the importance of particle size, spatial distribution, and standardized imaging strategies for accurate quantification and characterization. Future studies incorporating replicate samples and environmentally aged particles will further strengthen method validation under realistic environmental conditions.

REFERENCES

Al-Azzawi MSM, Kefer S, Weiser J, Reichel J, Schwaller C, Glas K, Knoop O, Drewes JE (2020) Validation of sample preparation methods for microplastic analysis in wastewater matrices – reproducibility and standardization. Water 12: 2445.

Andrady AL (2011) Microplastics in the marine environment. Mar Pollut Bull 62: 1596–1605.

Barnes DKA, Galgani F, Thompson RC, Barlaz M (2009) Accumulation and fragmentation of plastic debris in global environments. Philos Trans R Soc B 364: 1985–1998.

Berdutina AV, Neklyudov AD, Ivankin AI, Karpo BS, Mitaleva SI (2000) Comparison of proteolytic activities of the enzyme complex from mammalian pancreas and pancreatin. Appl Biochem Microbiol 36: 363–367.

Campanale C, Savino I, Massarelli C, Uricchio VF (2023) Fourier transform infrared spectroscopy to assess the degree of alteration of artificially aged and environmentally weathered microplastics. Polymers 15: 911.

Chen Y, Wen D, Pei J, Fei Y, Ouyang D, Zhang H, Luo Y (2020) Identification and quantification of microplastics using Fourier-transform infrared spectroscopy: Current status and future prospects. Curr Opin Environ Sci Health 18: 14–19.

Circelli L, Cheng Z, Garwood E, Yuksel K, Di Iorio E, Angelico R, Colombo C (2024) Comparison of ATR-FTIR and NIR spectroscopy for identification of microplastics in biosolids. Sci Total Environ 916: 170215.

Cole M, Lindeque P, Halsband C, Galloway TS (2011) Microplastics as contaminants in the marine environment: A review. Mar Pollut Bull 62: 2588–2597.

Cole M, Webb H, Lindeque PK, Fileman ES, Halsband C, Galloway TS (2014) Isolation of microplastics in biota-rich seawater samples and marine organisms. Sci Rep 4: 4528.

Cverenkárová K, Valachovičová M, Mackuľak T, Žemlička L, Bírošová L (2021) Microplastics in the food chain. Life 11: 1349.

Dehaut A, Cassone AL, Frère L, Hermabessiere L, Himber C, Rinnert E, Rivière G, Lambert C, Soudant P, Huvet A, Duflos G, Paul-Pont I (2016) Microplastics in seafood: Benchmark protocol for their extraction and characterization. Environ Pollut 215: 223–233.

Di Fiore C, Ishikawa Y, Wright SL (2024) A review on methods for extracting and quantifying microplastic in biological tissues. J Hazard Mater 464: 132991.

Duis K, Coors A (2016) Microplastics in the aquatic and terrestrial environment: Sources, fate and effects. Environ Sci Eur 28: 2.

Faszczewska A, Piotrowska-Niczyporuk A, Karpińska J (2026) Biodegradation of high-density polyethylene, polyethylene terephthalate, and polystyrene microplastics by bacteria, fungi and algae: A polymer-specific review. J Environ Sci. doi: 10.1016/j.jes.2026.01.087.

Fernández-Sanmartín P, Robledo-Mahón T, Requena-Menéndez A, Martínez-Cortizas A, Aranda E (2024) ATR-FTIR characterisation of daily-use plastics mycodegradation. Ecotoxicol Environ Saf 286: 117232.

Golmohammadi M, Musavi SF, Habibi M, Maleki R, Golgoli M, Zargar M, Dumée LF, Baroutian S, Razmjou A (2023) Molecular mechanisms of microplastics degradation: A review. Sep Purif Technol 309: 122906.

Hermsen E, Mintenig SM, Besseling E, Koelmans AA (2018) Quality criteria for the analysis of microplastic in biota samples: A critical review. Environ Sci Technol 52: 10230–10240.

Hidalgo-Ruz V, Gutow L, Thompson RC, Thiel M (2012) Microplastics in the marine environment: A review of the methods used for identification and quantification. Environ Sci Technol 46: 3060–3075.

Kalogerakis N, Karkanorachaki K, Kalogerakis GC, Triantafyllidi EI, Gotsis AD, Partsinevelos P, Fava F (2017) Microplastics generation: Onset of fragmentation of polyethylene films in marine environment mesocosms. Front Mar Sci 4: 84.

Karami A, Golieskardi A, Choo CK, Romano N, Ho YB, Salamatinia B (2017) A high-performance protocol for extraction of microplastics in fish. Sci Total Environ 578: 485–494.

Käppler A, Fischer D, Oberbeckmann S, et al (2016) Analysis of environmental microplastics by vibrational microspectroscopy: FTIR, Raman or both? Anal Bioanal Chem 408: 8377–8391.

Khan AL, Zaidi AA (2025) Separation and detection of microplastics in human exposure pathways: Challenges, analytical techniques and emerging solutions. J Xenobiot 15: 154.

Kovačić I, Štefanko K, Špada V, Pustijanac E, Buršić M, Burić P (2024) Microplastics in Mediterranean mussel *Mytilus galloprovincialis*: Comparison between cultured and wild-type mussels. Appl Sci 14: 2056.

Li J, Yang D, Li L, Jabeen K, Shi H (2015) Microplastics in commercial bivalves from China. Environ Pollut 207: 190–195.

Löder MGJ, Imhof HK, Ladehoff M, Löschel LA, Lorenz C, Mintenig S, Piehl S, Primpke S, Schrank I, Laforsch C, Gerdts G (2017) Enzymatic purification of microplastics in environmental samples. Environ Sci Technol 51: 14283–14292.

Lujic T, Mutic T, Simovic A, Vasovic T, Ivanovic S, Krstic-Ristivojevic M, Jovanović V, Cirkovic Velickovic T (2025) Protein corona stability and removal from PET microplastics: Analytical and spectroscopic evaluation in simulated intestinal conditions. Foods 14: 3454. doi: 10.3390/foods14203454.

Mihailov ME, Chiroşca AV, Pantea ED, Chiroşca G (2025) Machine learning approaches for microplastic pollution analysis in *Mytilus galloprovincialis* in the Western Black Sea. Sustainability 17: 5664.

Mintenig SM, Löder MG, Primpke S, Gerdts G (2019) Low numbers of microplastics detected in drinking water from ground water sources. Sci Total Environ 648: 631–635.

Mo Y, Li J, Jiang B, Su T, Geng X, Liu J, Jiang H, Shen C, Ding P, Zhong G, Cheng Z, Liao Y, Tian C, Chen Y, Zhang G (2018) Sources, compositions and optical properties of humic-like substances in Beijing during the 2014 APEC summit. Environ Pollut 239: 322–331.

Morgado V, Palma C, Bettencourt da Silva RJN (2021) Microplastics identification by infrared spectroscopy – Evaluation of identification criteria and uncertainty by the bootstrap method. Talanta 224: 121814.

Narayanan P, Janardhanan SK (2024) An approach towards identification of leather from leather-like polymeric material using FTIR-ATR technique. Collagen Leather 6: 1.

Pfeiffer F, Fischer EK (2020) Various digestion protocols within microplastic sample processing. Front Environ Sci 8: 572424.

Pizzurro F, Nerone E, Ancora M, Di Dominico M, Mincarelli LF, Camma C, Salini R, Di Renzo L, Di Giacinto F, Corbau C, Bokan I, Ferri N, Recchi S (2023) Exposure of *Mytilus galloprovincialis* to microplastics: Accumulation, depuration and evaluation of molecular biomarkers. Animals 14: 4.

Pizzurro F, Recchi S, Nerone E, Salini R, Barile NB (2022) Accumulation evaluation of potential microplastic particles in *Mytilus galloprovincialis* from the Goro Sacca (Adriatic Sea, Italy). Microplastics 1: 303–318.

Prata JC, Da Costa JP, Duarte AC, Rocha-Santos T (2019) Methods for sampling and detection of microplastics in water and sediment: A critical review. TrAC Trends Anal Chem 110: 150–159.

Schwab ST, Baur M, Nelson TF, Mecking S (2024) Synthesis and deconstruction of polyethylene-type materials. Chem Rev 124: 2327–2351.

Song J, Wang C, Li G (2024) Defining primary and secondary microplastics: A connotation analysis. ACS ES&T Water 4: 2330–2332.

Sunny AR, Sazzad SA, Islam MA, Mithun MH, Hussain M, Raposo A, Bhuiyan MKA (2025) Microplastics in aquatic ecosystems: A global review of distribution, ecotoxicological impacts and human health risks. Water 17: 1741.

Tirkey A, Upadhyay LSB (2021) Microplastics: An overview on separation, identification and characterization of microplastics. Mar Pollut Bull 170: 112604.

Turmanova S, Hristov Y, Kiryakova D, Ivanova E, Atanasova P, Kolchakova G, Ilieva A, Mollova E, Dimitrov A, Todorov N, Grigorova G (2026) Comparative evaluation of enzymatic, acidic and alkaline digestion protocols for organic matrix removal from lyophilized and frozen mussel samples (*Mytilus galloprovincialis*). Front Toxicol 8. doi: 10.3389/ftox.2026.1808944.

Tuuri EM, Gascooke JR, Leterme SC (2024) Efficacy of chemical digestion methods to reveal undamaged microplastics from planktonic samples. Sci Total Environ 947: 174279.

U.S. Environmental Protection Agency (2024) Microplastics research. http://www.epa.gov. Accessed 24 October 2024.

Van Cauwenberghe L, Devriese L, Galgani F, Robbens J, Janssen CR (2015) Microplastics in sediments: A review of techniques, occurrence and effects. Mar Environ Res 111: 5–17.

von Friesen LW, Granberg ME, Hassellöv M, Gabrielsen GW, Magnusson K (2019) An efficient and gentle enzymatic digestion protocol for the extraction of microplastics from bivalve tissue. Mar Pollut Bull 142: 129–134.

Yang H, Chen G, Wang J (2021) Microplastics in the marine environment: Sources, fates, impacts and microbial degradation. Toxics 9: 41.